Available online at www.sciencedirect.com
SCIENCE DIRECT®
ELSEVIER
Geomorphology 54 (2003) 63–75
GEOMORPHOLOGY
www.elsevier.com/locate/geomorph

Monitoring landslides from optical remotely sensed imagery: the case history of Tessina landslide, Italy

Javier Hervás[a,*], José I. Barredo[a], Paul L. Rosin[b], Alessandro Pasuto[c], Franco Mantovani[d], Sandro Silvano[c]

[a] *Institute for the Protection and Security of the Citizen, DG Joint Research Centre, European Commission, 21020 Ispra, Varese, Italy*
[b] *Department of Computer Science, Cardiff University, Newport Road, Cardiff CF24 3XF, UK*
[c] *Istituto di Ricerca per la Protezione Idrogeologica (IRPI)-CNR, Corso Stati Uniti 4, 35127 Padova, Italy*
[d] *Dipartimento di Scienze Geologiche e Paleontologiche, Università di Ferrara, Corso Ercole I° D'Este 32, 44100, Ferrara, Italy*

Received 29 November 2000; received in revised form 13 April 2001; accepted 3 January 2003

Abstract

Collecting information on landslide occurrence and activity over wide areas is a crucial task for landslide hazard assessment. Field techniques, despite being very precise, are usually not sufficient to achieve this goal, since they mostly provide point-based measurements. Mainly because of its synoptic view and its capability for repetitive observations, optical (visible-infrared) remotely sensed imagery acquired at different dates and at high spatial resolution can be considered as an effective complementary tool for field techniques to derive such information.

An image-processing method to map and monitor landslide activity using multitemporal optical imagery is proposed. The method entails automatic change detection of suitably pre-processed (geometrically registered and radiometrically normalised) sequential images, followed by thresholding into landslide-related change pixels. Subsequent filtering based on the degree of rectangularity of regions can also be considered to eliminate pixel clusters corresponding to man-made land use changes.

The application of this method is illustrated in the complex Tessina landslide in the Eastern Italian Alps. It has focused on discriminating the effects of a major reactivation that occurred in 1992, hence inferring the dynamics of the landslide at that time. Although the method has been devised for optical remote sensing imagery in general, in the absence of high-resolution satellite imagery covering that period, digital images derived by scanning existing aerial photograph diapositives at 1-m pixel size have been used. The method is able to classify image pixels according to landslide activity conditions.

Keywords: Landslide monitoring; Optical remote sensing; Change detection; Image thresholding; Northern Italy

1. Introduction

Monitoring landslide activity over extensive areas is of paramount importance for landslide hazard and risk assessment. Landslide monitoring is generally accomplished by field-based geodetic, geotechnical and geophysical techniques complemented with aerial

* Corresponding author. Institute for the Protection and Security of the Citizen, Joint Research Centre, European Commission, 21020 Ispra VA, Italy. Tel.: +39-0332-785229; fax: +39-332-789469.
E-mail address: javier.hervas@jrc.it (J. Hervás).

0169-555X/03/$ - see front matter © 2003 Elsevier Science B.V. All rights reserved.
doi:10.1016/S0169-555X(03)00056-4

photointerpretation (e.g. Mikkelsen, 1996; Keaton and DeGraff, 1996). Most field techniques, however, only provide point-based measurements of the landslides. In addition, they do not give information on past movement episodes. Although ground-based techniques are necessary to acquire very precise information on displacement or deformation at very specific locations in active landslides, especially when they might affect residential areas or major infrastructure, they do not provide information on the displacement fields or surface changes due to landsliding in a wider area. Moreover, their application to preliminary investigations of unstable areas may sometimes not be cost-effective.

From visual interpretation of sequential analogue aerial photo stereopairs, evidence of recent slope movements over relatively wide areas can often be inferred (Soeters and van Westen, 1996). This technique, although still useful, does not automatically and geometrically precisely determine the evolution of landslide features.

The capability of non-photographic remote sensing to provide information on ground surface conditions over extensive areas is well accepted. Differential synthetic aperture radar (SAR) interferometry from spaceborne platforms has been shown capable of measuring landslide displacement fields of centimetric order over relatively large areas (e.g. Fruneau et al., 1996; Massonnet and Feigl, 1998; Rott et al., 1999; Vietmeier et al., 1999). However, as these authors point out, its application is restricted to movements in the direction of the SAR antenna illumination, and may be frequently constrained by such factors as: loss of coherence between SAR data pairs in densely vegetated areas, unfavorable SAR illumination geometry with respect to slope aspect and angle, atmospheric effects and insufficient spatial resolution to cope with landslides with high internal deformation such as flows. In addition, both very slow and fast slope movements may not be resolved on radar data acquired over long time intervals.

Analytical and digital aerophotogrammetry has been used for measuring long-term landform evolution of rock glaciers and landslides from multitemporal digital elevation models (DEM) derived from sequential photo stereopairs (e.g. Brunsden and Chandler, 1996; Kääb et al., 1997). More recently, Kääb (2000) has also determined surface velocity vectors of metric order on a rockslide in a high alpine area using computer-aided aerial photogrammetry and correlation techniques. However so far, this method appears restricted to specific ground conditions including extensive rock outcrops and lack of major deformation within the landslide body.

Satellite remote sensing in the optical (visible-infrared) region of the electromagnetic spectrum, in turn, has been scarcely used for direct landslide monitoring. A major reason for this has been the insufficient spatial resolution provided until very recently by most spaceborne earth observation systems (Soeters and van Westen, 1996; Mantovani et al., 1996). On non-stereoscopic digital imagery, efforts have thus mainly concentrated on extracting possible indirect landslide indicators such as land cover disruption patterns, specific sun-shading features of hummocky surfaces and scarps and atypical lithological occurrence patterns (e.g. McKean et al., 1991; Hervás and Rosin, 1996; Hervás et al., 1996; Mason et al., 1998). The recent advent of IKONOS and Quickbird satellite imagery at very high spatial resolution, together with that soon to be delivered by similar missions, opens new perspectives for monitoring landslides.

As part of the RUNOUT project of the EU 4th Research Framework Programme on Natural Risks, an image processing method has been developed to map ground-surface changes caused by slope movements, using multitemporal high-resolution optical remotely sensed imagery. The method includes change detection and thresholding of suitably pre-processed images acquired before and after the slope movement episode. It could be applied over extensive areas in most common mountain landscapes to complement information derived from well-established field techniques. The proposed method has been applied to the Tessina landslide in Belluno province, Northeast Italy, where a number of documented reactivation episodes have occurred during the last decades (Pasuto et al., 1993; Angeli et al., 1994; Turrini et al., 1994; Mantovani et al., 2000). In particular, the latest major reactivation in 1992 has been analysed. Since high spatial resolution satellite imagery was not available at the time of this event, simulated IKONOS digital imagery at 1-m resolution from existing aerial photographs acquired between 1988 and 1994 has been used in this experiment.

2. Methodology

Using sequential optical imagery to map ground surface changes due to landsliding requires images to be both geometrically and radiometrically comparable on a pixel by pixel basis. Prior to applying specific change detection techniques, it is therefore necessary to remove, to the greatest possible extent, undesired effects on the images caused by sensor viewing geometry and relief, sun-illumination and sensor differences. Our landslide monitoring method has thus entailed the following image processing sequence.

2.1. Image orthorectification

Geometric distortions caused by viewing geometry, platform instability and earth curvature and rotation are common in spaceborne remotely sensed imagery. In mountainous areas, high altitude variations within the image frame introduce additional distortions. Except for the earth properties, these effects are augmented in airborne scanner imagery. On aerial photographs, in turn, major geometric distortions are due to their central projection and differences in terrain altitude.

To overcome these distortions, image orthorectification is applied. In order to correct for relief differences, a digital elevation model (DEM) is needed. Depending on the topography of the area and the spatial resolution of the imagery, an accurate DEM may be required. Such a DEM is not often available and may therefore need to be created. To this end, fast digital photogrammetry techniques can be applied to high-resolution stereo imagery (typically to aerial photographs) by optimising the strategy parameters (Gooch and Chandler, 1998; Chandler, 1999).

Pixel resampling to the new coordinate location is finally accomplished by assigning the nearest neighbour intensity value. In this way, no new pixel values are created prior to the radiometric normalisation process.

2.2. Radiometric normalisation

Differences in sun illumination (including also shadowing), atmospheric conditions and sensor/camera (and film, when analogue imagery is used) response may cause significant variations in pixel radiance values for a target on remotely sensed images acquired at different dates. These effects are usually higher between archived airborne images than for sun-synchronous satellite images. Aerial photographs, for example, are often available only from different seasons and from different times of day. Automatic analysis of land surface changes at pixel level on multitemporal raw images would therefore be greatly hampered by non-ground specific conditions.

On optical remote sensing images in general, these variation effects may be corrected either by absolute calibration of the single images or by pixel brightness normalisation between the images (Chuvieco, 1996). For aerial photographs, only the latter approach appears feasible. In our method, a relative radiometric normalisation procedure is performed for each orthoimage of the sequence with respect to a reference image. A simple equation can thus be applied to each orthoimage as follows.

$$NI[t_{n(x,y)}] = a_0 + a_1 \times I[t_{n+i(x,y)}]$$

where $NI[t_{n\ (x,y)}]$ are the pixel intensity values of the sequence orthoimage radiometrically normalised to those of the reference orthoimage, and $I[t_{n+i\ (x,y)}]$ are the pixel raw intensity values of the sequence orthoimage. a_0 and a_1 are the so-called bias and gain coefficients, which are derived from regression analysis between each image and the reference image, using pixel intensity values taken from approximately invariant ground targets (i.e. which are assumed not to change with time), such as asphalt and bare soil (Hall et al., 1991; Hill and Sturm, 1991).

2.3. Change detection

In remote sensing, a number of methods for land cover change detection are possible (Singh, 1989). In general, two basic approaches can be considered: either analysis of independently classified images (the so-called "post-classification" techniques) or simultaneous analysis of multitemporal images ("pre-classification" techniques) followed by thresholding to discard differences possibly related to non-surface changes (Singh, 1989; Eastman and McKendry, 1994). For panchromatic imagery, the latter approach appears more suitable. In this, although a number of image processing techniques can be applied to derive the

simple pixel intensity change image, it is usually accomplished either by image ratioing or, most frequently, image differencing.

Image ratioing involves a simple ratio operation between the values of corresponding pixels of two registered images of different dates (on a band-by-band basis if images are multispectral). With this operation, more weight is progressively given to pixel differences closer to zero. As a result, the numeric scale is neither symmetrical nor linear, thus making the subsequent thresholding process difficult. To facilitate thresholding, a log transformation can be applied to the ratio image, thus making the scale linear and symmetrical about zero. Image differencing in turn involves the subtraction of pixel values between both images. Unlike the ratio technique, the difference method highlights all cases of change to the same extent.

To map ground surface changes due to landsliding using radiometrically normalised, multitemporal remotely sensed orthoimagery, we have developed a method based on digital change detection techniques. The method encompasses two main steps: image differencing and subsequent thresholding into classes of changes in connection with landslide activity.

The thresholding procedure here is essential to discriminate "true change" image pixels by filtering out from the change image most of the noise due to scene changes between the image acquisitions and residual differential illumination and geometric misregistration effects.

A wide range of thresholding techniques has been reported by Sahoo et al. (1988), and considerable research continues nowadays (e.g. Chan et al., 1998; Dizenzo et al., 1998; Gong et al., 1998). Bilevel image thresholding into simple "change" and "no change" classes most often requires the occurrence of two distinct modes in the image intensity histogram. In addition, these two peaks should not be too similar in size and they should have approximately normal distributions. However, in change detection analysis of remotely sensed images over inland areas, the image histogram may often contain only one obvious peak, as is the case for the Tessina images. This causes difficulties for most popular thresholding algorithms (Rosin, 2002).

In order to correctly threshold difference images with unimodal histograms, a number of algorithms have been investigated on images of the Tessina area (Rosin et al., 2000). From these, we have selected a simple thresholding algorithm proposed earlier by Rosin (2001), which is specifically designed for unimodal histograms, and consists of thresholding at the corner of the histogram. To find this corner, a straight line is first drawn from the peak (largest bin) to the high end (first empty bin following the last filled bin) of the histogram (Fig. 1). The threshold point is selected at the pixel intensity value that maximises the perpendicular distance between the line and the histogram distribution. The distance along the perpendicular from a histogram point (x_i, y_i) to the line $(x_1, y_1) \rightarrow (x_2, y_2)$ is derived as follows.

$$\frac{(y_1 - y_2)x_i - (x_1 - x_2)y_i - x_2y_1 + x_1y_2}{\sqrt{(x_1 - x_2)^2 + (y_1 - y_2)^2}}$$

Not only is this algorithm simple and robust, but it has been shown to work effectively in a variety of applications such as edge, motion and texture thresholding.

The thresholding is applied to the absolute pixel difference values (i.e. negative values are made positive). The resulting binary image can then be classified into positive and negative categories of change by checking for each above threshold value the sign of the original signed difference image. Depending on the spectral characteristics of land cover and under-

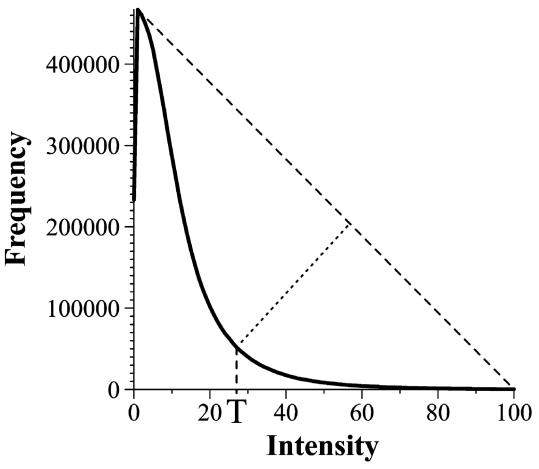

Fig. 1. Difference image histogram showing threshold value (T) corresponding to the detected corner.

lying soil/bedrock on unstable slopes, such a classification may enable a better identification and monitoring of slide masses.

Regardless of the preliminary thresholding algorithm applied to the difference image, it is assumed however that simple thresholding may often not be sufficient to identify true changes, in particular those due to landsliding. An additional processing step could then be applied to further filter out undesirable noise. Depending on the local properties and amount of scene noise still apparent after preliminary thresholding, some filters could be effectively applied. For instance, we could eliminate possible polygonal-shaped man-made features such as crop parcels, buildings and even road segments, as well as randomly distributed local changes in land use, since they do not typically correspond to effects of landslides. To this end, rectangularity filtering could be applied preceded by area filtering, so as not to measure very small pixel groups as perfectly rectangular (Rosin et al., 2000).

3. Case study

3.1. Physical setting and landslide dynamics

The methodology illustrated in this work has been applied to one of the test sites of the RUNOUT project. In particular, the Tessina landslide has been selected because of the availability of multitemporal aerial photographs and the large amount of data concerning recent major movements.

The landslide is located in the Alpago Basin, Eastern Italian Alps, in Belluno province, some 85-km north of Venice (Fig. 2). The Tessina landslide, which was first triggered in October 1960 following 1 month of abundant rainfall, is a complex movement with a source area affected by rotational and translational slides in the upper sector; downhill the slide turns into a mudflow through a narrow steep channel. The mudflow skimmed the village of Funès and stretched downhill as far as the village of Lamosano (Fig. 3).

During the 1960s, several reactivations occurred, involving about 5 million m^3 of material, causing the filling of the Tessina valley with displaced material from 30 to 50 m thick. These movements seriously endangered the village of Funès, which is situated on a steep ridge originally quite high above the river bed, but now nearly at the same level as the mudflow (Pasuto et al., 1993).

The landslide mainly involved the Flysch Formation (Eocene) consisting primarily of densely interbedded marls and sandstone with a thickness of about 1000–1200 m. This formation makes up the impermeable bedrock of the entire sliding area and crops out at the foot of Mt. Teverone, which is mainly made up of Fadalto Limestone (Cretaceous). The Flysch Formation appears strongly folded and fractured as a consequence of the intensive tectonic activity in the area, which is characterised by the occurrence of significant structural discontinuities. This has produced a high secondary permeability in the formation, thus helping the occurrence of numerous springs, especially in the landslide source area, some of these with perennial flow. Surficial Quaternary deposits including colluvium and glacial till have also been mobilised by the landslide.

The neighbouring area is covered mainly by alternating grassland and mixed woodland (coniferous and deciduous), with three small villages and scattered houses with orchards.

From a geomorphological standpoint, the Tessina landslide has a large source area with rotational slides and mudflows depositing the material onto a wide flat area making up the upper accumulation zone (Fig. 2). From here, and through a narrow and steep canal, the material feeds a thick flow downstream that has already filled up the valley and approaches the villages of Funès and Lamosano. The landslide developed in the Tessina valley between altitudes of 1220 and 625 m asl, with a total longitudinal extension of nearly 3 km and a maximum width of about 500 m.

In this work, we have focused on the application of our methodology to monitor ground surface changes due to a major reactivation of the landslide that occurred in April 1992. On that occasion, the easternmost part of the source area collapsed as a result of high precipitation and snow melting. This event affected mostly the eastern sector of the main scarp, which had not previously suffered significant movements. It involved an area of 40,000 m^2 with an approximate volume of 1 million m^3. This movement was a rotational slide with surface of rupture at an estimated depth of 20 or 30 m. This slide also involved the flysch substratum, causing initially a 15 m high main scarp and a downstream displacement of the area

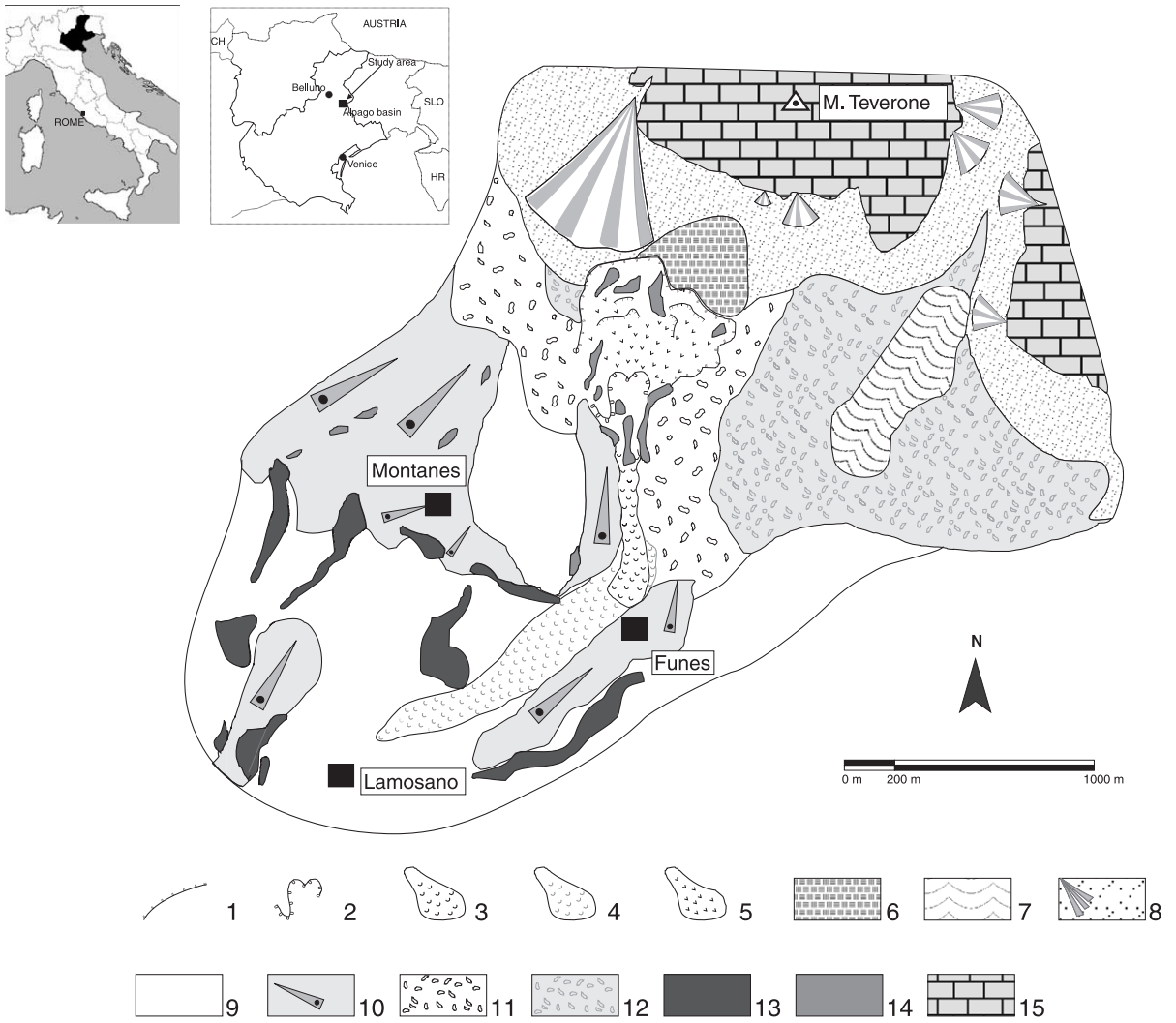

Fig. 2. Geomorphological sketch of the study area as of 2000. Legend: (1) Main landslide scarp; (2) secondary scarps; (3) active flow; (4) inactive flow; (5) rotational slide area; (6) recent fractured area; (7) rock glacier; (8) talus scree and talus cone; (9) eluvial and colluvial deposits; (10) glacis; (11) morainic deposit of the Piave glacier; (12) morainic deposit of the local glaciers; (13) molasse (Miocene); (14) Flysch Formation (Eocene); (15) Faldato Limestone (Cretaceous).

of nearly 100 m, followed by fragmentation and further sliding of the primary slide mass. Movements in this area continued until June 1992, affecting another 30,000 m^2 with an estimated total volume of 2 million m^3. The mobilised material, thus strongly fractured and loose, later displaced through the narrow stream valley where, because of continuous reworking and increase in water content, it became more fluid triggering small earth flows which subsequently fed the main mudflow body.

Following this event, a ground-based monitoring and alarm system was devised and installed, simultaneously with the realisation of control works in some urban settlements located along the valley, in order to mitigate the related risk (Pasuto et al., 1999).

3.2. Imagery used and pre-processing

The landslide monitoring method proposed was tested on digital panchromatic imagery simulating the

Fig. 3. Aerial view of the Tessina landslide and the threatened village of Funès in 1995.

1 m spatial resolution provided by the IKONOS orbiter. For this purpose, we used existing high-altitude black and white aerial photographs acquired on 28/9/88 and 7/10/94 at 1:75,000 scale, thus embracing the 1992 landslide reactivation period. These two images were preferred for comparative digital analysis to another available set of 31/8/89, because of their more similar vegetation and seasonal illumination conditions. High-quality photograph diapositives were precisely scanned at 8 bits and 14 μm, thus delivering 1-m pixels. Available aerial photographs from earlier years were not used to monitor previous major movements of the Tessina landslide, as they did not comply with photogrammetric requirements for accurate DEM extraction and image orthorectification, such as availability of contact diapositives and camera calibration data.

To digitally analyse multitemporal photographs obtained from different viewpoints, they must be orthorectified to remove relief distortions arising from the central projection. Such effects are noticeable on

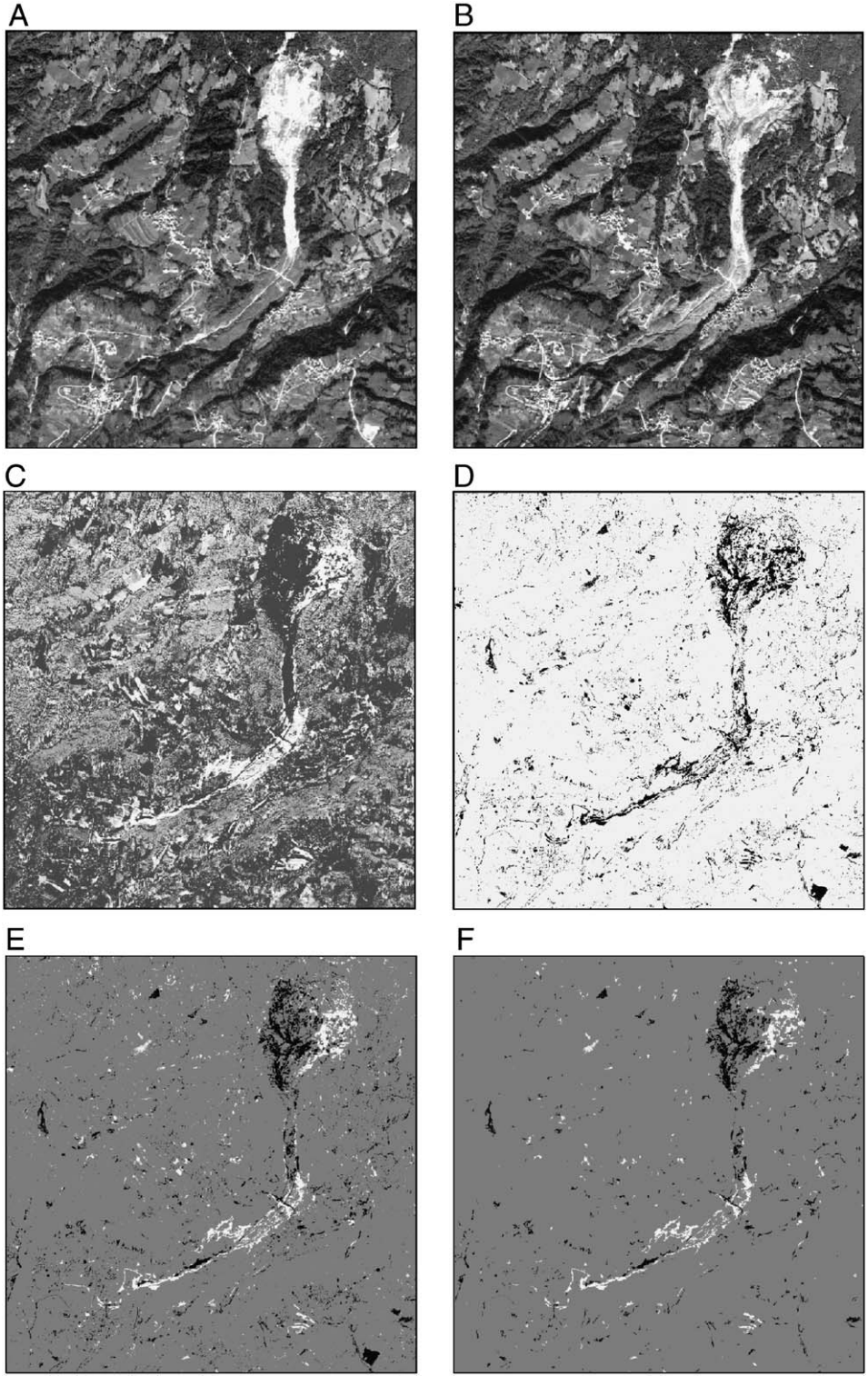
A
B
C
D
E
F

the Tessina images despite being taken from high-altitude flights. To this end, a DEM of the area was first generated. For this task, digital photogrammetric techniques were preferred to vectorising a number of 1:5000-scale monochromatic hardcopy topographic maps covering the study area.

The images of 31/8/89 were selected to create the DEM because of their lower shadowing affects with respect to the other dates. Ground control points (GCP) extracted from the above-mentioned maps were used to perform aerotriangulation using the Softplotter aerotriangulation model (Autometric, 1999). The accuracy so achieved (i.e. standard deviation of unit weight: 0.4; RMS: 3.3 m for X, 3.6 m for Y and 3.6 m for Z) was regarded acceptable, considering the ± 2.5-m accuracy of the GCPs used. Higher triangulation accuracy could have been possible using GPS differential measurements. The accuracy obtained however proved sufficient during the later orthorectification process. From the stereo-resampled images and triangulation results, a raster DEM at a resolution of 20 m was derived. For Tessina, this resolution was shown to be adequate to produce well-registered orthophotographs.

Orthorectification was first accomplished for one of the photographs of 31/8/89 (used for generating the DEM) by applying a geometric transformation using the 20-m grid DEM values and pixel positions resulting from the triangulation process. Orthoimages were produced from photographs of 28/9/88 and 7/10/94 using the same DEM and the 31/8/89 orthophoto as reference for GCP collection. Sub-pixel accuracy was thus achieved in the orthorectification process of the relatively small area common to both the aerial photographs and the DEM.

Next, the pixel intensity values of the 7/10/94 orthophotograph were normalised to those of the 28/9/88 orthophotograph following the procedure described earlier (Fig. 4a and b). For the Tessina images, bias and gain coefficients resulting from the regression analysis were 26.655 and 0.7482, respectively. Main statistical parameters for all the images are shown in Table 1. As a result of normalisation, the mean of the corrected 1994 orthoimage became almost equal to that of the 1988 orthoimage. However, statistical differences are still apparent. These can mainly be explained by land cover changes between the two dates including those owing to mass movements. Minor contribution from remnant differential illumination and geometric misregistration effects may also be possible. Both the 1988 and the normalised 1994 orthoimages can now be digitally compared to investigate changes caused by landsliding.

Table 1
Main statistics of the Tessina orthophotographs before and after radiometric normalisation

Aerial orthophotograph	Mean	Standard deviation	Min	Max
28/09/88 (reference)	90.72	29.98	34	250
07/10/94 raw	85.71	33.22	28	255
07/10/94 radiometrically normalised	90.33	24.82	47	217

3.3. Mapping ground surface changes related to landsliding

To map ground surface changes as a result of reactivation of the Tessina landslide and of other mass movements in the vicinity during the 1988-1994 period, the image change detection method previously described was applied to the normalised orthophotographs of these two dates. The method entailed: (1) the creation of an image expressing the differences in pixel brightness between the two input images (Fig. 4c), (2) preliminary thresholding of such an image using the histogram corner algorithm (Rosin, 2001) (Fig. 4d), (3) splitting the thresholded image into positive changes (i.e. increase in pixel brightness from the older image to the newer one) and negative changes (i.e. decrease in pixel brightness) (Fig. 4e) and (4) filtering out rectangular-shaped image blobs (that is, clusters of adjacent pixels) (Fig. 4f).

Step (3) enabled discrimination between new soil outcrops (positive pixel brightness changes) and new or growing vegetation patches during the elapsed period (negative pixel brightness changes). These two classes

Fig. 4. Change detection in Tessina landslide from digital aerial photography. (A) 18/9/88 orthophotograph; (B) radiometrically normalised 7/10/94 orthophotograph; (C) histogram-equalised difference image; (D) binary change image derived from histogram-corner thresholding the difference image; (E) previous image differentiating positive pixel intensity changes in white and negative changes in black; (F) additional blob filtering using area and rectangularity properties (see Fig. 5 for interpretation).

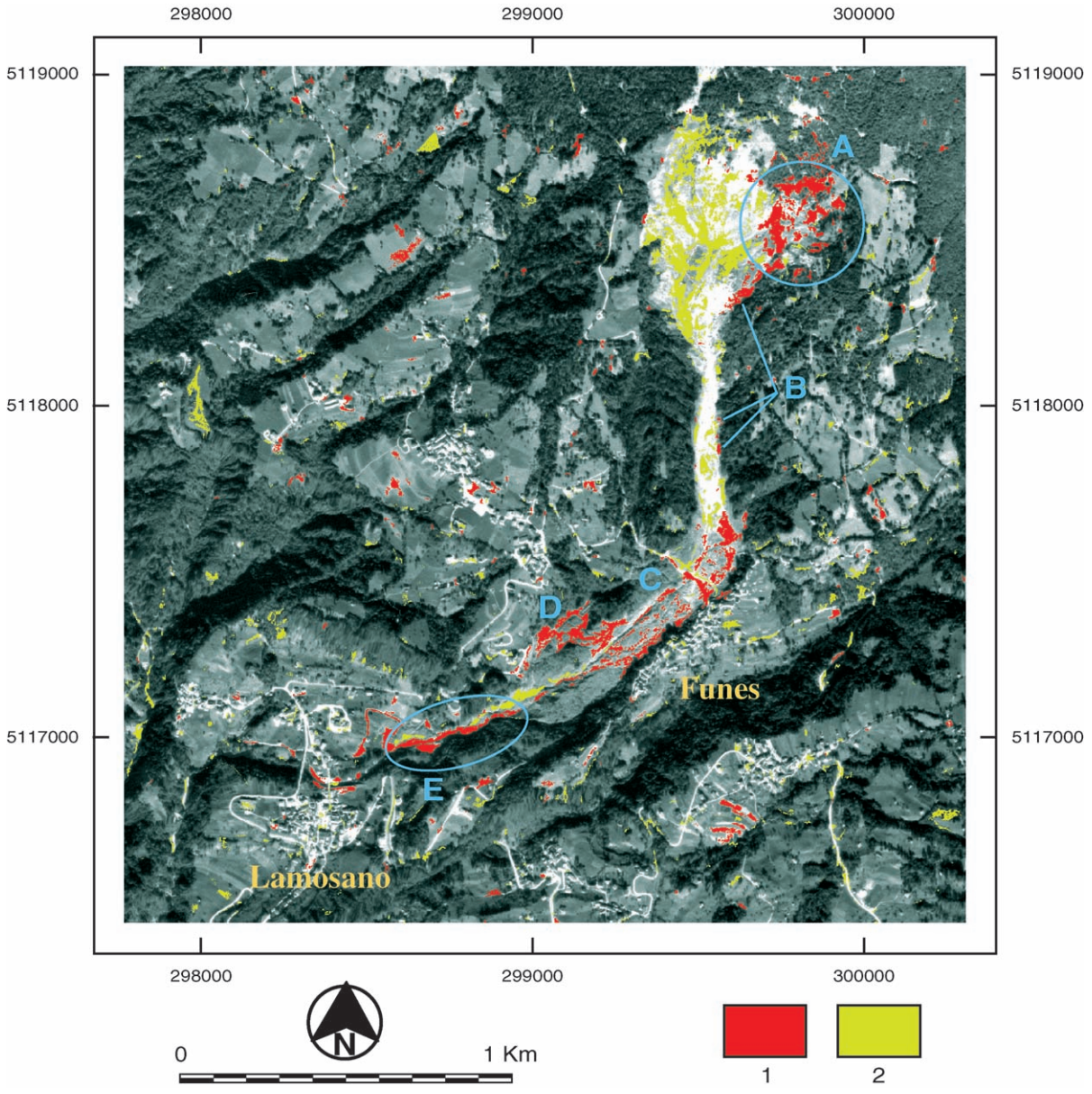

Fig. 5. Surface changes in the Tessina landslide between 1988 and 1994 illustrated on the 1994 orthophotograph. Legend: (1) within the landslide body, positive pixel intensity changes represent both new soil outcrops and remobilised soil as a result of landslide reactivation; zones highlighted are explained in the text; (2) negative pixel intensity changes due to vegetation growth or soil moisture increase. Most changes outside the landslide correspond to land use change. Coordinates in UTM.

could generally be assumed for Tessina to be associated to ground instability and stability conditions, respectively (Fig. 5). Pixels with practically unchanged values in both images represent stable areas. They were eliminated during the first two processing steps above.

Step (4) helped to remove some undesired remnant change blobs simply representing land use or vegetation growth changes in polygonal-shaped crop parcels, as well as those due to new houses and new straight road segments. A suitable rectangularity threshold

value was selected using the unimodal thresholding scheme described earlier (Rosin, 2001). After area filtering to remove small blobs, a cumulative histogram was constructed which describes the number of blobs retained as a function of the rectangularity threshold. The detected "corner" of the histogram plot (Fig. 1) has been found to be a suitable rectangularity threshold setting (Rosin et al., 2000).

3.4. Discussion of results

The final result of the image processing sequence is shown in Fig. 5. Here, positive pixel intensity changes are colored in red. Within the Tessina landslide body, these represent ground change patterns mostly associated with the reactivation occurred in 1992, as documented by Pasuto et al. (1993) and Angeli et al. (1994), and illustrated by both on-site photographs and low-altitude aerial photographs taken at the time of such a reactivation. Five major change zones can be observed. First, the zone detached in 1992 from the northeastern landslide crown, which produced a landslide surface increase of 40,000 m^2 (zone A in the figure), thus showing fresh soil outcrops with higher pixel intensity in the 1994 image. New soil outcrops together with fresh remobilised material can also be observed along the flanks of the narrow steep canal (zone B) because of remobilisation and depletion of the previous mudflow in this zone and subsequent minor sliding of the main flanks. Zone C, adjacent to Funès, appears irregularly reworked by small mudflows and remobilisation of the former mudflow, as well as by man-made drainage channels (depicted as linear blobs) dug following the 1992 event. Zone D shows a mudflow running off the right flank of the landslide body, opposite to the village of Funès. Here, the higher brightness fresh slide mass partly filled a vegetated small depression originally made up by a side stream, after breaching a levee. Much of the former mudflow zone southwest of Funès appears, however, not affected by the 1992 movements. In this zone, the remobilised material, already highly fluidised, was funneled along the previously dug central drainage channel into the narrower valley section below, near the village of Lamosano, where the new runout material is clearly shown (zone E). New linear structures consisting of protection walls and concrete partly paving the Tessina stream floor, built in 1992, are also apparent at the north end of Lamosano because of their significant pixel brightness increase in the 1994 image.

Areas in yellow, which represent negative pixel intensity changes, appear mostly associated with either soil moisture increase or simple land cover changes, including the growth of natural vegetation on temporarily stable sectors of the landslide body. While vegetation growth may be an indicator of ground stability, soil moisture conditions (which can change dramatically over short periods of time) may conceal the brightness properties of the underlying ground, especially on panchromatic images. However, if a landslide sector is known to be bare of vegetation, thresholded negative brightness changes could indicate high risk of further movement. Vegetation indices derived from high-resolution multispectral imagery (e.g. Bannari et al., 1995) can be used for this purpose.

As shown in the figure, the ground area detached during the 1992 movement (zone A) could not be fully mapped using some automatic change detection techniques. This pattern may be explained by the high resemblance between the original land cover and that of some slide blocks at some locations. Since further erosion, consolidation and sliding processes have made the bench-like structure of the main scarp (as induced by the 1992 movement) greatly disappear, it is assumed that by comparative analysis of later images, most of that zone would appear filled with positively changed pixels meaning remobilised ground.

Because of the long time elapsed between the photographic shots, some remobilised zones within the landslide body could appear as "negative" changes (i.e. meaning stability) as a consequence of vegetation growth during the stability period comprised between the 1992 movement and the 1994 image take.

Numerous changes are also apparent throughout the area, away from the Tessina landslide. For instance, vegetation regrowth on stable sectors of gully sides can be seen northwest of Lamosano. Some recently mapped small rotational landslides in this zone (Pasuto et al., 1999) could not be inferred, since there was no sign of activity on the images during the study period. Most changes portrayed outside Tessina, however, correspond to land use changes. It can also be noticed that the final rectangularity-filtering step was not able to remove those with irregular shape still remaining after preliminary thresholding of the difference image,

while it overfiltered some change blobs in the source area of the landslide. Overall, it produced a cleaner change image, while retaining most significant surface changes caused by the landslide. The method also worked particularly well in woodland areas, where SAR interferometry and aerophotogrammetric techniques cannot usually be applied.

4. Conclusions

A method for mapping new landslide occurrence and monitoring ground surface changes (mainly land cover and exposed soil conditions) related to landslide activity using optical remotely sensed imagery has been proposed. The method is based on automatic digital image change detection and thresholding techniques. It has been successfully applied to high spatial resolution multitemporal imagery of the large and complex Tessina landslide in Northeastern Italy. In the absence of suitable satellite imagery covering a major reactivation episode, this has been simulated using small-scale black-and-white digital aerial photographs digitised at 1-m pixel size.

The method can be applied to monitor landslide occurrence and activity over extensive areas at scales up to 1:10,000 when using the latest generation of satellite imagery, thus complementing more precise point-based measurements provided by geodetic, geotechnical and GPS techniques, as well as visual photointerpretation. It is particularly useful for monitoring surface changes caused by moderate-velocity landslides, even if involving high internal deformation, in humid and heavily vegetated areas, where the application of more accurate radar interferometry techniques is often not possible. Unlike the latter techniques, this method does not need to process, and therefore to acquire, too many images to generate a useful product. In addition, since images are optical, such a product can be more easily interpreted by geomorphologists and other landslide analysts and engineers. As the method can be applied to aerial photographs, it is unique to monitor past landslide activity in unstable areas during the last decades.

Although the usefulness of the method has been demonstrated on panchromatic images separated by long time intervals, typically more frequent observations would be needed to more precisely monitor ground surface dynamics. This constraint is expected to be partly overcome by the new generation of high-resolution satellite systems, starting with IKONOS and Quickbird. In addition, the multispectral imaging capabilities to be provided by some of these systems will help to better discriminate surface changes exclusively due to slope movements. Finally, image-processing techniques should be used with caution on digital aerial photographs since, unlike most images acquired by satellite or airborne scanners, pixel values are not calibrated.

A major research effort, however, will still be needed to derive landslide movement rates from optical satellite imagery in a broad range of landslide scenarios. Strategies for the integrated use of optical remote sensing and SAR interferometry methods should also be investigated.

Acknowledgements

This research has been partly funded by the European Commission's Research DG under the FP4 Environment and Climate Programme, Natural Risks, RUNOUT project (A. Ghazi, head of unit; M. Yeroyanni, scientific officer). Thanks are also due to Peter Spruyt of the Joint Research Centre, for helping generating the DEM. Digital aerial photographs were provided by CGR, Parma, Italy.

References

Angeli, M.-G., Gasparetto, P., Menotti, R.M., Pasuto, A., Silvano, S., 1994. A system of monitoring and warning in a complex landslide in Northeastern Italy. Landslide News 8, 12–15.

Autometric, 1999. SoftPlotter User's Guide, v2.0 Bangor, Maine, USA.

Bannari, A., Morin, D., Bonn, F., Huete, A.R., 1995. A review of vegetation indices. Remote Sensing Reviews 13, 95–120.

Brunsden, D., Chandler, J.H., 1996. Development of an episodic landform change model based upon the Black Ven mudslide, 1946–1995. In: Anderson, M.G., Brooks, S.M. (Eds.), Advances in Hillslope Processes. Wiley, Chichester, UK, pp. 869–896.

Chan, F.H.Y., Lam, F.K., Zhu, H., 1998. Adaptive thresholding by variational method. IEEE Transactions on Image Processing 7 (3), 468–473.

Chandler, J., 1999. Effective application of automated digital photogrammetry for geomorphological research. Earth Surface Processes and Landforms 24, 51–63.

Chuvieco, E., 1996. Fundamentos de Teledetección Espacial, tercera edición revisada Rialp, Madrid, Spain.

Dizenzo, S., Cinque, L., Levialdi, S., 1998. Image thresholding using fuzzy entropies. IEEE Transactions on Systems, Man and Cybernetics. B 28 (1), 15–23.

Eastman, J.R., McKendry, J.E., 1994. Change and time series analysis. Explorations in GIS Technology, vol. 1. UNITAR, Geneva, Switzerland.

Fruneau, F., Achache, J., Delacourt, C., 1996. Observation and modelling of the Sant-Etienne-de-Tinée landslide using SAR interferometry. Tectonophysics 265, 181–190.

Gong, J.A., Li, L.Y., Chen, W.N., 1998. Fast recursive algorithms for 2-dimensional thresholding. Pattern Recognition 31 (3), 295–300.

Gooch, M.J., Chandler, J.H., 1998. Optimization of strategy parameters used in automated digital elevation model generation. In: Donoghue, D.N.M. (Ed.), Int. Archives of Photogrammetry and Remote Sensing. ISPRS, Data Integration: Systems and Techniques, Cambridge, vol. XXXII(2), pp. 88–95.

Hall, F.G., Strebel, D.E., Nickenson, E., Goetz, S.J., 1991. Radiometric rectification: toward a common radiometric response among multidate multisensor images. Remote Sensing of Environment 35, 11–27.

Hervás, J., Rosin, P.L., 1996. Landslide mapping by textural analysis of Daedalus ATM data. Proc. Eleventh Thematic Conf. Applied Geologic Remote Sensing, Las Vegas, Nevada, vol. 2. ERIM, Ann Arbor, Michigan, USA, pp. 394–402.

Hervás, J., Rosin, P.L., Fernández-Renau, A., Gómez, J.A., León, C., 1996. Use of airborne multispectral imagery for mapping landslides in Los Vélez district, south–eastern Spain. In: Chacón, J., Irigaray, C., Fernández, T. (Eds.), Landslides. Balkema, Rotterdam, pp. 353–361.

Hill, J., Sturm, B., 1991. Radiometric correction of multitemporal Thematic Mapper data for use in agricultural land-cover classification and vegetation monitoring. International Journal of Remote Sensing 12, 1471–1491.

Kääb, A., 2000. Photogrammetry for early recognition of high mountain hazards: new techniques and applications. Physics and Chemistry of the Earth 25 (9), 765–770.

Kääb, A., Haeberli, W., Gudmundsson, G.H., 1997. Analysing the creep of mountain permafrost using high precision aerial photogrammetry: 25 years of monitoring Gruben Rock glacier, Swiss Alps. Permafrost and Periglacial Processes 8, 409–426.

Keaton, J.R., DeGraff, J.V., 1996. Surface observation and geologic mapping. In: Turner, A.K., Schuster, R.L (Eds.), Landslides Investigation and Mitigation, Transportation Research Board Special Report 247. National Research Council, Washington D.C., pp. 178–230.

Mantovani, F., Soeters, R., van Westen, C.J., 1996. Remote sensing techniques for landslide studies and hazard zonation in Europe. Geomorphology 15, 213–225.

Mantovani, F., Pasuto, A., Silvano, S., Zannoni, A., 2000. Data collection aiming at the definition of future hazard scenarios of the Tessina landslide. International Journal of Applied Earth Observation and Geoinformation 2 (1), 33–40.

Mason, P.J., Rosenbaum, M., Moore, J.McM., 1998. Digital image texture analysis for landslide mapping. In: Maund, J.G., Eddleston, M. (Eds.), Geohazards in Engineering Geology. Engineering Geology Special Publications, vol. 15. Geological Society, London, pp. 297–305.

Massonnet, D., Feigl, K.L., 1998. Radar interferometry and its application to changes in the earth's surface. Reviews of Geophysics 36 (4), 441–500.

McKean, J., Buechel, S., Gaydos, L., 1991. Remote sensing and landslide hazard assessment. Photogrammetric Engineering and Remote Sensing 57 (9), 1185–1193.

Mikkelsen, P.E., 1996. Field instrumentation. In: Turner, A.K., Schuster, R.L. (Eds.), Landslides Investigation and Mitigation, Transportation Research Board, Special Report 247, National Research Council, Washington DC, pp. 278–316.

Pasuto, A., Silvano, S., Bozzo, G.P., 1993. The Tessina landslide (Belluno, Italy). In: Panizza, M., Soldati, M., Barani, D. (Eds.), Proc. First European Intensive Course on Applied Geomorphology, Pubblicazioni Istituto di Geologia, Universitá degli Studi di Modena, Italy, pp. 63–69.

Pasuto, A., Silvano, S., Tecca, P.S., Zannoni, A., 1999. Convenzione tra la Regione del Veneto e l' IRPI-CNR per lo studio della frana del Tessina in Comune di Chies d'Alpago (BL). Relazione finale. IRPI-CNR, Padova, Italy.

Rosin, P.L., 2001. Unimodal thresholding. Pattern Recognition 34 (11), 2083–2096.

Rosin, P.L., 2002. Thresholding for change detection. Computer Vision and Image Understanding 86 (2), 79–95.

Rosin, P.L., Hervás, J., Barredo, J.I., 2000. Remote sensing image thresholding for landslide motion detection. Proc. 1st Int. Workshop on Pattern Recognition Techniques in Remote Sensing, Andorra, 10–17.

Rott, H., Scheuchl, B., Siegel, A., Grasemann, B., 1999. Monitoring very slow slope movements by means of SAR interferometry: a case study from a mass waste above a reservoir in The Otztal Alps, Austria. Geophysical Research Letters 26, 1629–1632.

Sahoo, P.K., Soltani, S., Wong, A.K.C., Chen, Y.C., 1988. A survey of thresholding techniques. Computer Vision, Graphics and Image Processing 41, 233–260.

Singh, A., 1989. Digital change detection techniques using remotely sensed data. International Journal of Remote Sensing 10, 989–1003.

Soeters, R., van Westen, C.J., 1996. Slope instability recognition, analysis and zonation. In: Turner, K., Schuster, R.L. (Eds.), Landslides Investigation and Mitigation, Transportation Research Board, Special Report 247, National Research Council, Washington DC, pp. 129–177.

Turrini, M.C., Abu-Zeid, N., Semenza, E., Semenza, P., El-Naqa, A., 1994. New studies on the Tessina landslide (Belluno, Italy). Proc. 7th Int. IAEG Congress. Balkema, Rotterdam, pp. 1667–1675.

Vietmeier, J., Wagner, W., Dikau, R., 1999. Monitoring moderate slope movements (landslides) in the southern French Alps using differential SAR interferometry. Proc. 2nd Int. Workshop on ERS SAR Interferometry "FRINGE'99". Liege, Belgium.